Journal of Advanced Research xxx (xxxx) xxx

Contents lists available at ScienceDirect

Journal of Advanced Research

journal homepage: www.elsevier.com/locate/jare

Original Manuscript

TaWAK5 perceives OGs to activate drought responses in wheat

Jingyi Wang [a,*,1], Long Li [a,1], Chaonan Li [a,1], Matthew Reynolds [b], Manuel Spannagl [c], Jörg-Peter Schnitzler [d], Yang Zhao [a], Zilong Ma [a], Jiemeng Xu [b], Xinguo Mao [a], Ruilian Jing [a,*]

[a] State Key Laboratory of Crop Gene Resources and Breeding/Institute of Crop Sciences, Chinese Academy of Agricultural Sciences (CAAS), Beijing 100081, China
[b] International Maize and Wheat Improvement Center, Texcoco 56237, Mexico
[c] Plant Genome and Systems Biology (PGSB), Helmholtz Center Munich-German Research Center for Environmental Health, Neuherberg 85764, Germany
[d] Research Unit Environmental Simulation, Institute of Biochemical Plant Pathology, Helmholtz Zentrum München GmbH, Neuherberg 85764, Germany

HIGHLIGHTS

- *TaWAK5* is associated with wheat detached-leaf water loss rate.
- *TaWAK5* perceives drought-induced pectin fragments (OGs), triggering stomatal closure.
- Promoter SNP-947 affects *TaWAK5* expression and transcription factor TaPAN binding.

GRAPHICAL ABSTRACT

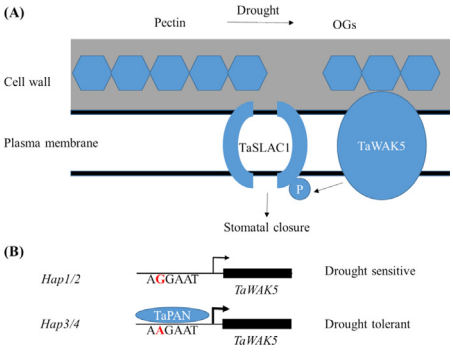

ARTICLE INFO

Article history:
Received 16 March 2025
Revised 5 March 2026
Accepted 7 March 2026
Available online xxxx

Keywords:
Wheat
WAK5
OGs
Drought
Detached-leaf water loss

ABSTRACT

Introduction: Numerous studies have elucidated plants' drought response, yet how plant leaves perceive this stress remains unclear.
Objectives: This study aims to deepen the understanding of how leaves perceive and respond to water loss.
Methods: Detached-leaf water loss rate was detected, which can effectively eliminate the effects of water absorption and water transport. Subsequently, a genome-wide association study (GWAS) was carried out on the detached-leaf water loss rate.
Results: There was a significant association between the *TaWAK5* (*cell wall-associated kinase*) gene and the detached-leaf water loss rate. Phenotypic analyses of overexpression and CRISPR/Cas9-based knockout lines revealed the function of TaWAK5 in wheat response to drought stress. Subsequent study exhibited that drought induced the degradation of pectin into oligogalacturonides (OGs), and OGs have a higher affinity for TaWAK5 than pectin does. OGs can activate TaWAK5 kinase, leading to stomatal closure. Additionally, TaWAK5 phosphorylates TaSLAC1 (slow anion channel-associated 1), a key component regulating stomatal movement. A single nucleotide polymorphism site SNP-947 (G/A), at 947 bp of the *cis*-element in the *TaWAK5* promoter region, is significantly associated with *TaWAK5* expression, detached-

* Corresponding authors.
E-mail addresses: wangjingyi@caas.cn (J. Wang), jingruilian@caas.cn (R. Jing).
[1] These authors contributed equally to this work.

https://doi.org/10.1016/j.jare.2026.03.018

Please cite this article as: J. Wang, L. Li, C. Li et al., TaWAK5 perceives OGs to activate drought responses in wheat, Journal of Advanced Research, https://doi.org/10.1016/j.jare.2026.03.018

leaf water loss rate and canopy temperature, and leads to the bZIP transcription factor TaPAN (PERIANTHIA) functioning as a transcriptional activator in haplotype *Hap3/4*, but not in *Hap1/2* of *TaWAK5*.

Conclusion: This study suggests that TaWAK5 perceives OGs to activate drought responses in wheat, highlighting a potential target for enhancing the drought tolerance of wheat.

Introduction

Wheat (*Triticum aestivum* L.) holds the distinction of being the most extensively grown crop across the globe. It supplies approximately 19% of the total calories that people consume worldwide [1,2]. As the global demand for food keeps rising and abiotic stresses like drought become more severe, it is urgent to explore the stress tolerance mechanisms in wheat in order to breed new cultivars with high and stable yields [3–5].

Plant cell walls are closely associated with stress responses, which comprise a variety of polymer compounds, including cellulose, hemicellulose, and pectin [6–8]. Among them, pectin is a complex polygalacturonic acid, which is mainly composed of 300 to 1000 galacturonic acid units (oligogalacturonides, OGs) connected by $\alpha 1 \rightarrow 4$ linkages [9]. The characteristics of pectin molecules, including length and degree of esterification, are of vital importance in numerous biological processes. These processes span from plant growth and pathogen defense responses to sensing high salinity-induced disruptions [10–13]. Moreover, both experimental data and computational modelling have demonstrated that the status of pectin also significantly influences the guard cell's stomatal development and movement [14,15]. For instance, in *POLYGALACTURONASE INVOLVED IN EXPANSION3* overexpression plants, pectin degradation enhances its fluidity, leading to accelerated stomatal movement [16]. Observations of stomata in *Arabidopsis thaliana* mutants lacking normal pectin have revealed that reducing pectin molecular mass results in enhanced stomatal opening [17]. Pectin degradation underlines stomatal pore formation [18]. Additionally, the methylesterification of pectin at the polar region modulates cell wall stiffness and limits the opening of maize stomata [19].

Cell wall-associated kinases (WAKs) belong to the receptor-like protein kinase family, which is composed of three parts: cytoplasmic serine/threonine kinase domain, transmembrane domain and extracellular domain connected to the pectin fraction of the cell wall [20,21]. WAKs were initially characterized by their strong affinity for the cross linked pectin component within the cell wall [22]. Subsequent studies have indicated the affinity of WAKs for OGs is significantly higher compared to that for longer pectin polymers [23–25]. WAKs not only regulate cell expansion in various developmental processes, but also get involved in defending against pathogens through sensing various pectin states [26–31]. Additionally, several studies have indicated WAKs participate in responding to wounding, aluminum stress, salt stress and dehydration [32–36]. WAKs have been detected in diverse plant species, such as *Arabidopsis*, *Brachypodium*, rice, maize, barley and cotton [37–45]. In wheat, TaWAK2A-800 and TaWAK7 participate in the pathogen response [46,47]. Nonetheless, the role that WAKs play in the drought response of wheat is still mostly unclear [48].

Maintaining an appropriate water balance is essential for plants to function optimally [49]. The water balance process mainly consists of the water uptake, transport and transpiration. In this study, we analyzed the detached-leaf water loss rate of wheat varieties. On the premise of eliminating the impacts of water absorption and water transport, we achieved an in-depth understanding of how plants sense and cope with water loss.

Results

Genome-wide association study (GWAS) revealed that TaWAK5 is associated with detached-leaf water loss rate

A wheat panel comprising 323 accessions was employed to assess the detached-leaf water loss rate at various time points following leaf detachment. The average detached-leaf water loss rate was 0.835 times of dry weight at 2 h, 1.99 times at 6 h, 3.27 times at 12 h, and 5.11 times at 24 h (Fig. S1). The detached-leaf water loss rates at different time intervals exhibited a significant positive correlation, with Pearson correlation coefficients ranging from 0.815 to 0.978 (Fig. 1A). The detached-leaf water loss rate was subsequently utilized as the phenotype for genetic analysis (Table S1). Through GWAS, several peaks where phenotypes were significantly correlated with genotypes were identified. Remarkably, a SNP on chromosome 5A was significantly associated with detached-leaf water loss rate at 6 h, 12 h, and 24 h (Fig. 1B).

The SNP that showed a significant association was located in the intron region of *TraesCS5A02G043600* (Fig. 1C). This gene encodes a wall-associated kinase (WAK) that is highly homologous to *Arabidopsis* WAK5. Consequently, the wheat gene is henceforth designated as *TaWAK5* (Fig. S2). WAKs were reported to participate in various stress responses [30]. This suggests that *TaWAK5* is a candidate gene regulating detached-leaf water loss.

TaWAK5 is involved in wheat drought tolerance

To confirm TaWAK5′s function, *TaWAK5* overexpression and knockout lines were created. Two high *TaWAK5* expression lines (OE3 and OE6, Fig. S3), and two CRISPR/Cas9-based *TaWAK5* knockout lines which were edited only in genome A (*tawak5-1* and *tawak5-2*, Fig. S4) were chosen for analysis. The survival rates of these seedlings under drought condition were examined. After withholding water for 25 days followed by 5 days of re-watering, the survival rates of *tawak5-1* and *tawak5-2* seedlings were 13.3% and 10.7%, respectively, compared with 26.7% for wild-type Fielder and 53.9% and 60.0% for overexpression lines, respectively (Fig. 2A, B). Moreover, the detached-leaf water loss rate was the highest in *tawak5-1*, *tawak5-2* lines, and higher in Fielder compared with that in *OE3* and *OE6* (Fig. 2C). Correspondingly, following 14 days of drought treatment, the stomatal aperture on the leaf abaxial epidermis of *tawak5-1*, *tawak5-2* seedlings at the three-leaf stage was the largest, and larger in Fielder compared with that of the *OE*s (Fig. 2D). Under drought stress condition, the 1000-grain weight of *OE* lines was the highest, and that of *tawak5-1* and *tawak5-2* lines was the lowest compared with Fielder (Fig. 2E). However, no significant difference was observed in other yield-related traits, such as spike number per plant, grain number per spike under well-watered or drought stress conditions (Fig. S5).

TaWAK5 activity is regulated by OGs in response to drought treatment

Previous studies proposed WAKs establish a connection between the cytoplasm and the extracellular matrix [36,50]. To investigate the protein localization of TaWAK5, we constructed a

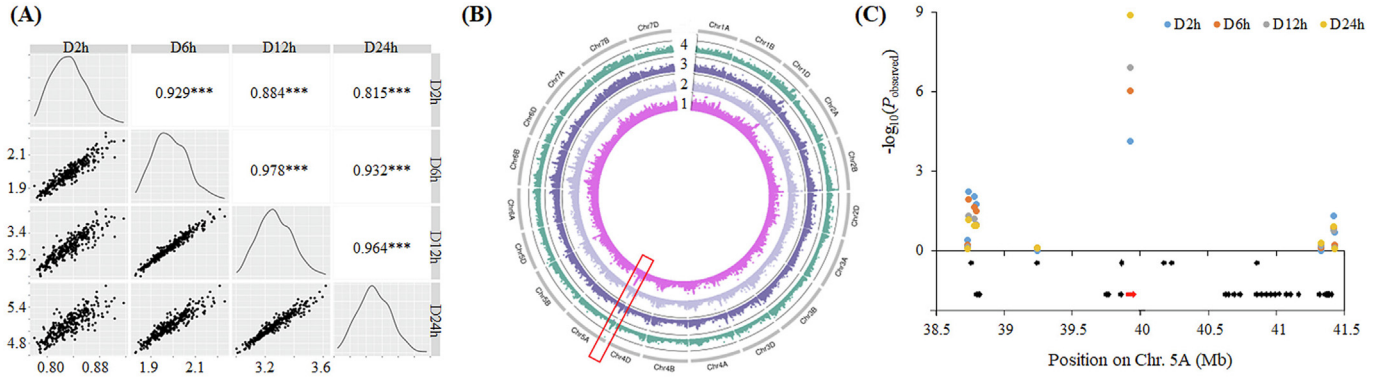

Fig. 1. GWAS identified a locus on chromosome 5A showing a significant association with detached-leaf water loss rate. **(A)** Correlation and frequency distributions of the detached-leaf water loss rate. The X axis and Y axis represent the detached-leaf water loss rate. The bottom left section depicts scatter plots of detached-leaf water loss rate in 323 accessions. The upper right section depicts the correlation coefficients of detached-leaf water loss rate at different time points. The diagonal panels display frequency distribution plots. D2h, D6h, D12h, D24h represent the detached-leaf water loss rate at 2 h, 6 h, 12 h and 24 h post leaf detachment, respectively. ***, $P < 0.001$. **(B)** GWAS results for the detached-leaf water loss rate based on the mixed linear model (MLM). Numbers 1, 2, 3, and 4 indicate the GWAS results at time points 2 h, 6 h, 12 h, and 24 h, respectively. The significance threshold adjusted by the Bonferroni method is denoted by gray circular lines. It is set at $P = 2.53 \times 10^{-6}$, which is equivalent to 1 divided by 395,675. Red rectangle indicates the focused locus in this study. **(C)** Manhattan plot of the region around the *TaWAK5* genomic locus (38.7 – 41.4 Mbp). The SNPs detected at various time points are shown by colored dots. The peak SNP is located in the *TaWAK5* intron region. The arrows indicate the Gene models (IWGSC_v1.1). The red arrow indicates the location of *TaWAK5* (*TraesCS5A02G043600*).

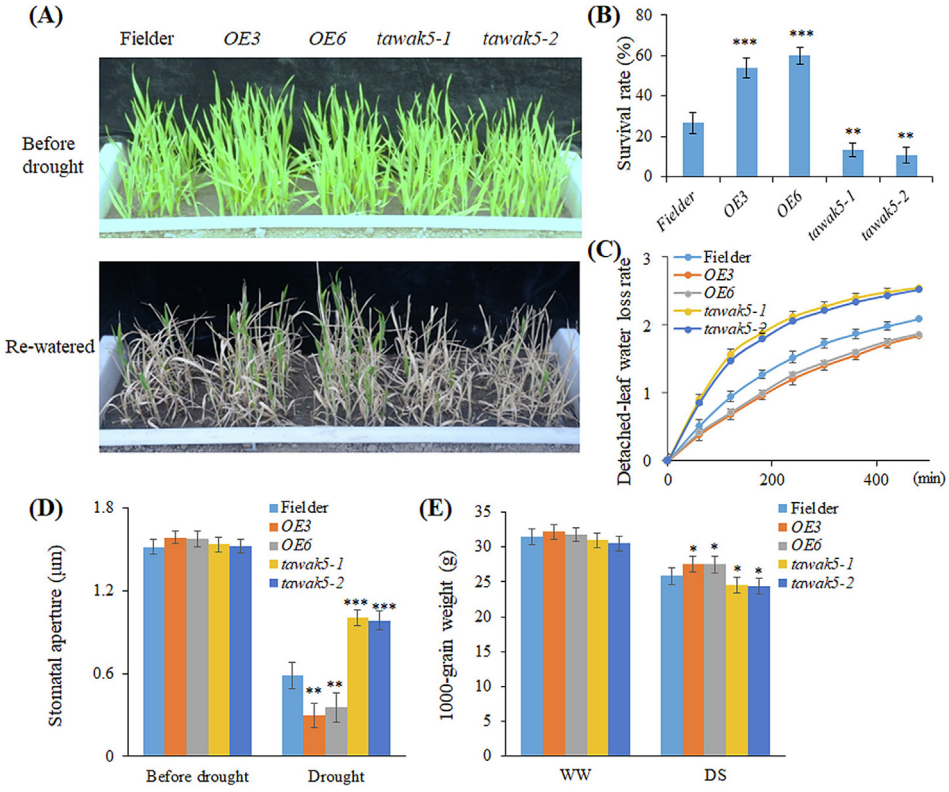

Fig. 2. Phenotypic characteristics of *TaWAK5* overexpression and knockout lines. **(A)** The seedlings of wild type Fielder, *OE3*, *OE6*, *tawak5-1* and *tawak5-2* before drought, and after drought followed by re-watering treatments. Three-leaf stage seedlings underwent a 25-day drought treatment and subsequently re-watered. Photo was taken on the fifth day following re-watering. **(B)** Seedling survival rates after re-watering. Survival rate is the percentage of seedlings that grow new leaves after rehydration relative to the total number of seedlings prior to the drought treatment. **(C)** Detached-leaf water loss rate. Leaves from three seedlings were collected and weighed at predetermined time intervals. **(D)** Stomatal aperture was measured on the abaxial epidermis of the second fully expanded leaf before and after a 14-day drought treatment. A minimum of 30 stomata were assessed per replicate, and all experiments were conducted in triplicate. **(E)** Thousand grain weight comparison. Plants were cultivated under both well-watered (WW) and drought stress (DS) conditions in two growing seasons of 2022 and 2023. Error bars, ± SE. *, *t*-test with $P < 0.05$. **, *t*-test with $P < 0.01$. ***, *t*-test with $P < 0.001$.

TaWAK5-GFP fusion protein. Fluorescence signals were observed at the cell boundaries in *Nicotiana benthamiana* leaves expressing TaWAK5-GFP (Fig. 3A). Following plasmolysis, fluorescence signals were localized to the plasma membrane, cell wall and extracellular matrix (Fig. 3B). However, in cells expressing the GFP alone, fluorescence was restricted to the cytoplasm and plasma membrane. These results indicate TaWAK5 localizes to the plasma membrane, cell wall and extracellular matrix, and it has the potential to bind to extracellular molecules, and may be involved in signaling cellular events.

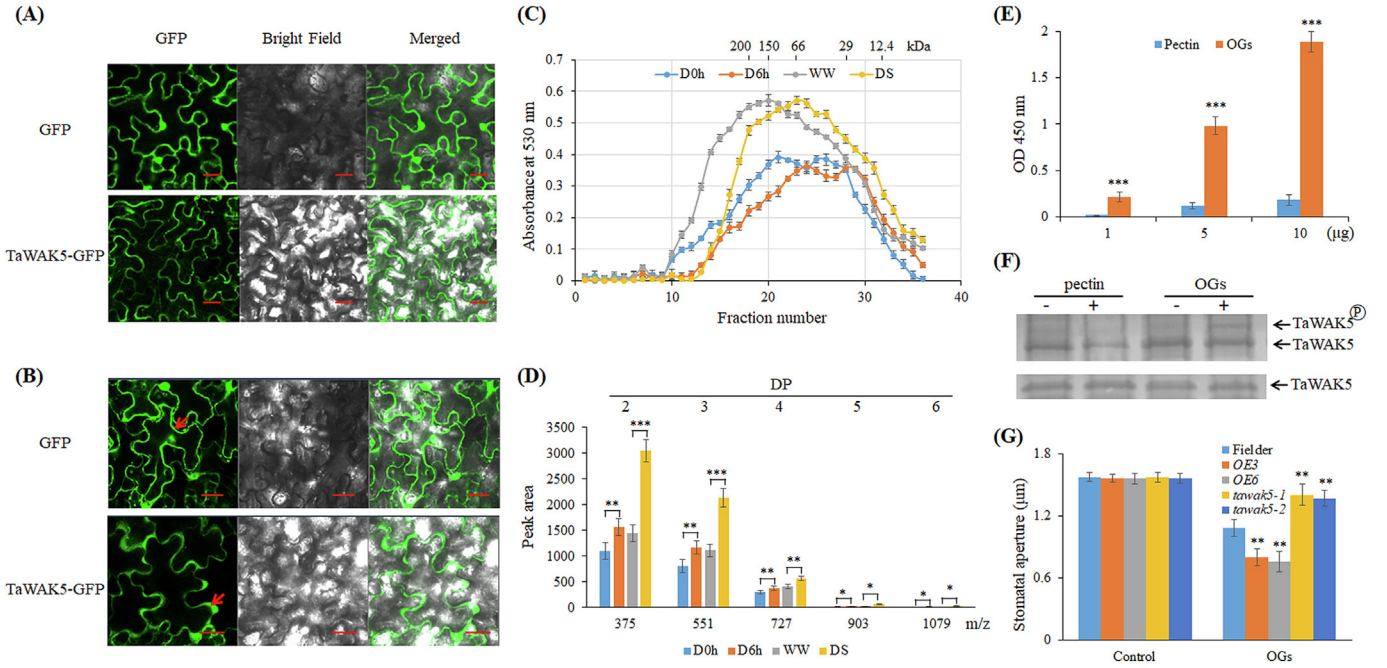

Fig. 3. TaWAK5 responds to drought treatment and its activity is regulated by OGs. **(A, B)** Subcellular localization of TaWAK5 in tobacco leaves. **(A)** Photos of cells before mannitol treatment. **(B)** Photos of plasmolysed cells. Images were taken following a 10 min incubation of the samples in a 0.8 M mannitol solution. Red arrows denote the plasma membrane of plasmolysed cell. Bars, 20 μm. **(C)** Molecular mass profile of pectin in Fielder leaves at the three-leaf stage under detached or drought stress treatments. D6h represents samples detached for 6 h, while D0h represents the original state of detached samples. DS (drought-stressed) represents samples treated by water deprivation for 2 weeks, and WW (well-watered) represents samples cultivated under well-watered conditions. The mean ± SE was obtained from three replicates. **(D)** OGs levels with degrees of polymerization (DP, ranging from 2 to 6) in wheat samples under different treatments were analyzed by MALDI-TOF mass spectrometry. The X-axis represents the mass-to-charge ratio (m/z) corresponding to DP 2–6. The Y-axis indicates the peak area. **(E)** ELISA assay of recombinant TaWAK5 N-terminal domain interacting with pectin and OGs. The OD 450 nm reflects the TaWAK5-N domain remaining attached to the coated pectin or OGs, as detected using an anti-GST antibody. The mean ± SE was obtained from three replicates. **(F)** Autophosphorylation assays of TaWAK5 protein under pectin or OGs treatment. The upper anti-GFP Western blot analysis of the Phos-tag polyacrylamide gel showed the autophosphorylated and non-autophosphorylated TaWAK5-GFP. The lower anti-GFP Western blot analysis of polyacrylamide gel indicated that a similar amount of TaWAK5-GFP protein was utilized. **(G)** Stomatal aperture of the abaxial epidermis of the second fully expanded leaf either before or under 1 h treatment with OGs. A minimum of 30 stomata were assessed per replicate, and all experiments were conducted in triplicate. Error bars, ± SE. Statistical significance was determined by a two-sided *t*-test, * $P < 0.05$, ** $P < 0.01$, *** $P < 0.001$.

Plants infected with pathogen can release OGs from the cell walls, and these OGs can then trigger defense responses [51]. Additionally, mechanical stimuli, such as touch, can also modulate the molecular mass of pectin polymers [11]. Therefore, the effect of drought on the pectin molecular mass was examined using fast protein liquid chromatography. The peak of the pectin polymers in detached 6-hour (D6h) leaves of Fielder seedlings appeared at fraction #24. In contrast, the peak in leaves detached for 0 h (D0h) occurred at fraction #21 (Fig. 3C). This suggests that the molecular mass of pectin was decreased by the detached treatment. Furthermore, the polymers peak of the leaves of the three-leaf seedlings treated with water deprivation (drought-stressed, DS) for 2 weeks was observed at fraction #23, while that of the leaves of the seedlings with well-watered (WW) appeared at fraction #20 (Fig. 3C), indicating that the molecular mass of pectin in the leaves decreases due to drought treatment. OGs levels were further quantified by matrix-assisted laser desorption/ionization time-of-flight mass spectrometry (MALDI-TOF). The contents of OGs with degrees of polymerization (DP) ranging from 2 to 6 in D6h leaves were significantly higher than that in D0h leaves (Fig. 3D). Similarly, OGs levels were elevated in DS leaves compared to WW counterparts (Fig. S6). These results suggest that drought can induce pectin degradation and the release of OGs.

Previous studies suggested the N-terminal of WAKs can bind pectin, but its affinity with OGs is stronger than that of pectin [23–25]. We expressed and purified TaWAK5 N-terminal in vitro (Fig. S7). Binding of the TaWAK5 N-terminal to pectin or OGs was examined through enzyme-linked immunosorbent assay (ELISA) [23,38]. The results showed that TaWAK5 exhibited dose-dependent interactions with pectin and OGs. Moreover, TaWAK5 displayed a much higher binding affinity for OGs compared with pectin (Fig. 3E).

OGs can activate the WAK kinase activity and trigger the pathogen defense response in plants [52,53]. Hence, we investigated whether the protein kinase activity of TaWAK5 is regulated by OGs. Tobacco leaves expressing TaWAK5-GFP were treated with OGs or pectin, and subsequently, the TaWAK5 protein was detected using an anti-GFP antibody. Upon treatment with OGs, autophosphorylated TaWAK5 was detected. In contrast, almost no autophosphorylated TaWAK5 was observed after treatment with pectin (Fig. 3F). This indicated that OGs enhance the kinase activity of TaWAK5. Compared with Fielder treated with OGs for 1 h, the stomatal aperture in the abaxial epidermis of the *tawak5-1* and *tawak5-2* lines significantly increased, while that of *OEs* significantly decreased (Fig. 3G). The results showed that exogenous OGs can induce stomatal closure in wheat, with the most pronounced effect on *TaWAK5* overexpression lines and the least effect on knockout lines, suggesting *TaWAK5* responds to the OGs treatment.

TaWAK5 interacts with and phosphorylates TaSLAC1

As shown in Fig. 2D, TaWAK5 exerts a significant influence on the stomatal aperture under drought conditions. Consequently, we examined the interaction of TaWAK5 with several known ABA signaling components, including TaPYL4, TaPP2C158,

TaSnRK2.10 and TaAREB3, aiming to identify the phosphorylation substrate of TaWAK5 via the bimolecular fluorescence complementation (BiFC) assay [54–58]. The results demonstrated a robust YFP signal when TaSLAC1-YCE and TaWAK5-YNE were co-expressed (Fig. 4A), suggesting that TaWAK5 could interact with TaSLAC1 (SLOW ANION CHANNEL-ASSOCIATED1), which is an S-type anion channel as a key component in regulating stomatal movement, and its knockdown lines slowed down the reduction of stomata apertures following drought stress [59–61]. The interaction between TaWAK5 and TaSLAC1 was further verified through Co-immunoprecipitation (CoIP) assay (Fig. 4B). The proteins TaWAK5-C (consisting of amino acids 381–715), TaSLAC1-N (consisting of amino acids 1–194) and TaSLAC1-C (comprising amino acids 509–575) were purified from *Escherichia coli* for in vitro phosphorylation assay and Phos-tag mobility shift assay. The results showed that only TaSLAC1-N was phosphorylated when co-incubated with TaWAK5-C and ATP (Fig. 4C). These results suggested that TaWAK5-C can interact with and phosphorylate TaSLAC1-N, rather than with TaSLAC1-C.

TaPAN regulates the expression of TaWAK5 via binding to the promoter region of Hap3/4

To further explore whether genetic variation in *TaWAK5* is correlated with differences in the detached-leaf water loss rate, we extracted the *TaWAK5* sequence (a 16.1 kb genomic region encompassing the promoter and coding region) from 36 chromosome-assembled wheat accessions sourced from the WheatOmics website and then analyzed the sequence polymorphism [62,63]. A total of 102 polymorphic loci were identified. Based on 2 polymorphic loci, i.e. the SNP at –947 bp (A/G, for which a dCAPS molecular marker was designed) and the SNP at 12,580 bp (C/T, AX-109929811 of Wheat 660 K SNP Array), the natural population consisting of 323 wheat accessions was categorized into 4 haplotypes (Fig. 5A, Fig. S8, Table S2). Notably, genotypes carrying haplotype *Hap1* and *Hap2* with SNP-947-G exhibited significantly higher detached-leaf water loss rates compared to those carrying haplotype of *Hap3* and *Hap4* with SNP-947-A (Fig. 5B). Considering that SNP-947 is situated within the promoter region of *TaWAK5*, we speculated that it might influence the expression of *TaWAK5*. The test results demonstrated that the expression of *TaWAK5* in SNP-947-A genotypes was significantly higher than those in SNP-947-G genotypes (Fig. 5C), indicating that the SNP-947 affects the expression of *TaWAK5*.

Through the Plant Transcription Factor Database (https://planttfdb.cbi.pku.edu.cn/), we identified *cis*-element variations among the four haplotypes. A PAN (PERIANTHIA) protein binding site (AAGAAT) was detected at 947 bp upstream of the ATG translation start site in *Hap3/4*. In contrast, this binding site was not present in *Hap1/2* because of the A to G variation (*Hap1/2*: AGGAAT, *Hap-3/4*: AAGAAT) (Fig. 5D). *PAN*, a gene that encodes a bZIP-transcription factor, was reported to modulate redox homeostasis or responses [64].

Yeast one-hybrid assays were performed to verify whether TaPAN binds to the promoter region of *TaWAK5*. The TaPAN was fused into the pB42AD vector. *Hap1/2* and *Hap3/4* fragments from the *TaWAK5* promoter region of Fielder and Chinese Spring were cloned into pLacZi, respectively (Fig. 5D). TaPAN was found to bind and activate the LacZ reporter gene when the *TaWAK5* promoter region from *Hap3/4* is present, but not when the *TaWAK5* promoter region from *Hap1/2* is present (Fig. 5E). The results suggested that TaPAN specifically binds to the *Hap3/4* promoter rather than the *Hap1/2* promoter, which can be attributed to the difference in *cis*-elements (SNP-947). This difference might result in varying expression levels of *TaWAK5* haplotypes. Furthermore, dual luciferase (LUC) assay demonstrated that in the presence of the TaPAN effector, the LUC activity with the *TaWAK5 Hap3/4* promoter reporter constructs was higher than that with *Hap1/2* constructs (Fig. 5F). These findings imply that TaPAN functions only as a transcriptional activator for *TaWAK5* from *Hap3/4* and not for that from *Hap1/2*.

The previous studies have shown that SNP-947 has a significant effect on detached-leaf water loss rate, so we further investigated its effects on the relevant physiological traits of the wheat panel of 323 accessions. As depicted in Fig. 5G, the canopy temperature of wheat accessions with SNP-947-A was significantly lower than that of accessions with SNP-947-G in 13 out of 20 environments.

Discussion

Stomatal transpiration is the main way of water loss in plant leaves. The detached-leaf water loss rate assay provides a straightforward method to evaluate the water retention capacity of the leaves by measuring the weight of detached leaves. This method eliminates the need to consider variations in water absorption and transport within plants. GWAS has revealed that *TaWAK5* is highly associated with the detached-leaf water loss rate. It was discovered that drought can induce the production of low-molecular-OGs, and TaWAK5 exhibits a higher affinity with OGs compared to longer pectin polymers, and these OGs can activate TaWAK5 kinase activity and prompt stomatal closure.

Challenges in identifying primary drought stress sensors

Drought can directly cause numerous physical and chemical alterations in biomolecules within plant cells, initiating a series of stress responses [65,66]. Therefore, identifying the primary drought stress sensors is highly challenging. Multiple methods have been employed to uncover the primary sensors of drought stress [67,68]. A comprehensive review has summarized both membrane macromolecules (such as nuclei, plasma membranes, endoplasmic reticulum) and membraneless macromolecules (such as stress granules, speckles, and those involved in liquid–liquid phase separations) that have the ability to sense and signal abiotic stress [69–71]. Previous studies mainly focused on how roots sense water shortage in the soil and then transfer this signal to the above-ground tissues to trigger drought tolerance [72–79]. Our results suggest that OGs from plant leaf cell walls could be considered as a potential signaling molecule of drought stress.

Role of OGs as signaling molecules

During pathogen infection or wounding, OGs can be released from the cell wall, perceived by WAKs, and activate plant immunity or mechanical wounding responses, thus serving as plant damaged-associated signaling components [33,52,80,81]. Short OGs have also been regarded as a type of dark-related signal for regulating the elongation of hypocotyl in plant during photomorphogenesis [82]. Additionally, an interaction between FERONIA (FER) and pectin was observed in *Arabidopsis*, indicating that FER might be able to detect cell-wall properties, and pectin fragments (potentially OGs) could act as sensors during salt stress [13]. Our study demonstrated that OGs can induce stomatal closure in wheat leaves, suggesting OGs play a universal role as signaling molecules. However, it remains to be investigated how plants distinguish these various stresses and trigger different responses through OGs [83]. One potential explanation is that different receptors might recognize varying lengths of OGs, leading to distinct responses.

Pectin dynamics in drought adaptation

Pectin status plays a fundamental role in plant drought responses. Pectin characteristics, including polymer length and esterification degree, influence guard cell development and movement [14–18]. Recent studies reveal that polar-enriched methylesterified pectin

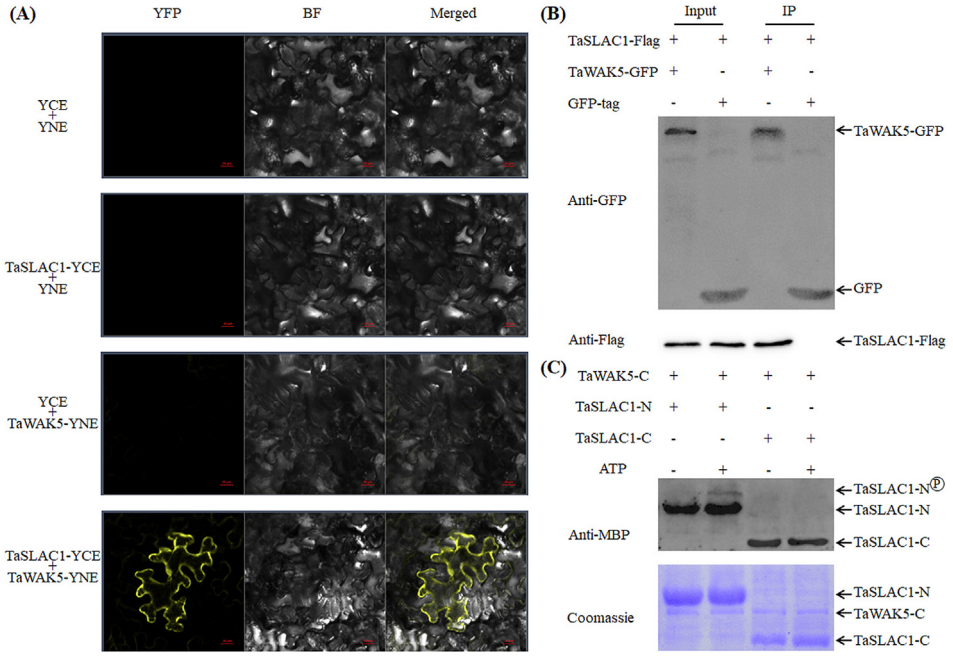

Fig. 4. TaWAK5 interacts with and phosphorylates TaSLAC1. **(A)** The interaction between TaWAK5 and TaSLAC1 was identified via bimolecular fluorescence complementation (BiFC) assay. Bars, 20 μm. **(B)** CoIP of TaWAK5 with TaSLAC1. TaWAK5-GFP and TaSLAC1-Flag were co-expressed in tobacco leaves. After precipitating protein with anti-GFP magnetic beads, immunoblotting assays with anti-Flag antibodies were carried out. **(C)** In vitro phosphorylation assay and Phos-tag mobility shift assay. The TaSLAC1-N and TaSLAC1-C proteins tagged with MBP, as well as the TaWAK5-C protein tagged with GST were purified and co-incubated with or without ATP to perform the in vitro phosphorylation assay. Immunoblotting detection indicated that only TaSLAC1-N was phosphorylated in the presence of TaWAK5-C and ATP, whereas TaSLAC1-C could not be phosphorylated. Polyacrylamide gel was stained by Coomassie brilliant blue R250 as control.

modulates wall stiffness and limits maize stomatal opening [19]. Evolutionarily, increased pectin concentration enhances leaf drought tolerance by improving cell wall flexibility in dry forests [84]. Our findings add another dimension: drought-induced pectin degradation produces OGs that activate TaWAK5 signaling for stomatal closure. Thus, pectin dynamics, such as polymer length, methylesterification status, evolutionary concentration, or degradation products, may all contribute to plant drought adaptation.

Relationship between Ca^{2+} and OGs signaling

In addition to being recognized as a drought stress signaling molecule, Ca^{2+} has also been proven to be involved in pectin-related processes [68,72]. The binding of Ca^{2+} ions with the pectin backbone promotes the formation of calcium bridges (known as “egg box” structure) [85]. Additionally, through Ca^{2+} signaling, FER has been observed to interact with pectin to sense high salinity stress [13]. The interaction between WAKs and cell wall pectin is dependent on Ca^{2+} [23]. Therefore, the relationship between Ca^{2+} and OGs signaling, and how they crosstalk with each other requires further study.

Conclusion

Overall, our findings suggest that TaWAK5 is of significant importance in wheat leaf sensing drought stress. Through its extracellular domain, TaWAK5 is capable of sensing the dynamic changes occurring in the cell wall and delivering this signal into the cell through the cytoplasmic kinase domain.

Materials and methods

Growth conditions and detached-leaf water loss rate assay

The wheat plants were cultivated in containers (80 cm × 40 cm × 20 cm, length × width × height) under a removable rain-off shelter until three-leaf stage, as described previously [56]. All leaves were cut from 3 seedlings of each accession and placed on weighing paper. The leaves were placed at room temperature and under 30% relative humidity, and then weighed at predetermined time intervals. The percentage of leaf water loss relative to leaf dry weight was calculated as detached-leaf water loss rate [86]. Three biological replicates were performed.

GWAS of detached-leaf water loss rate

A wheat panel of 323 accessions, previously genotyped using the Wheat 660 K SNP Array, was used for GWAS of detached-leaf water loss rate [87,88]. GWAS between genotype and phenotype was performed as previously described using TASSEL 5.0 software based on the mixed linear model (MLM) combined with the kinship (K) and population structure (Q), using the best linear unbiased prediction (BLUP) approach.

Phylogenetic tree construction for WAK

The full-length amino acid sequence of TaWAK5-A was utilized as a query. By conducting a BLAST search of proteins in the NCBI database, members of the WAK family were identified across diverse plant species. Homologous WAKs were then aligned with the aid of DNAMAN. To construct a phylogenetic tree, the full-length proteins were processed using the maximum likelihood method implemented in the Molecular Evolutionary Genetics Analysis (MEGA) software, version 5.2.

Analysis of TaWAK5 protein structure

Transmembrane region in the TaWAK5 protein was predicted through DeepTMHMM (https://services.healthtech.dtu.dk/services/DeepTMHMM-1.0/).

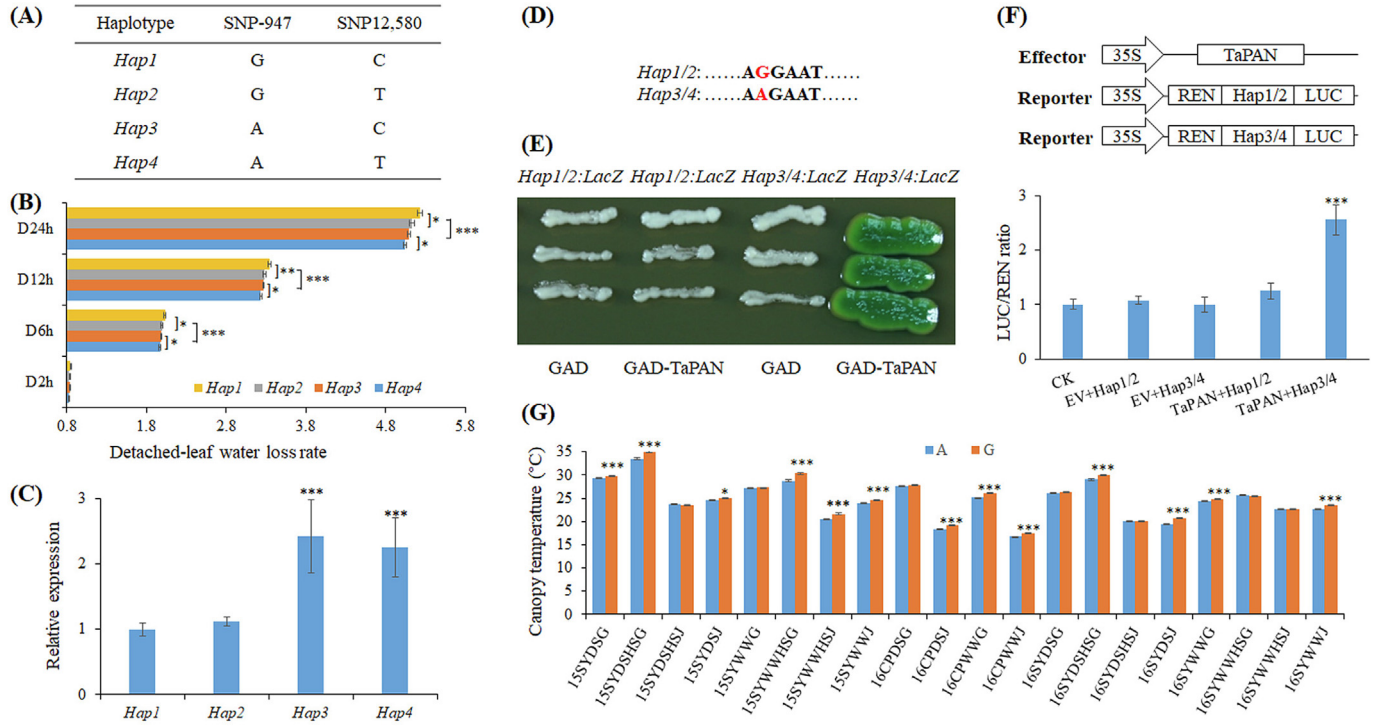

Fig. 5. TaPAN binds to the *TaWAK5 Hap3/4* promoter region. **(A)** Four *TaWAK5* haplotypes were identified in the wheat panel of 323 accessions. **(B)** Detached-leaf water loss rate of four haplotypes when the leaf was detached at 2, 6, 12, 24 h (D2h, D6h, D12h, D24h). **(C)** Comparison of *TaWAK5* expression among four haplotypes. **(D)** *Cis*-element differences between *Hap1/2* and *Hap3/4* promoter. The letters in red represent the SNP-947 (G/A) sites. **(E)** The expression of LacZ reporter gene was activated by GAD-TaPAN when it was driven by the *Hap3/4* promoter, rather than the *Hap1/2* promoter. **(F)** Dual-luciferase assays were performed on transformed tobacco leaves to investigate the interaction between TaPAN and *TaWAK5* promoter. Agrobacteria stains containing pSoup with reporter and effector constructs or an empty vector (EV) were co-infiltrated into tobacco leaves. The upper part shows the schematic representations of the effector and reporter constructs employed in the dual LUC assay. *TaPAN* was inserted into the effector construct pCAMBIA1300. The promoter fragments from *Hap1/2* or *Hap3/4* were separately cloned into the reporter vector pGreen II 0800-LUC. Renilla luciferase (REN) served as a control for normalizing the activity. The lower part shows the promoter activities, presented as the ratio of LUC to REN. **(G)** Comparisons of canopy temperature in the wheat panel comprising 323 accessions under 20 environments: grown during 2014–2015 and 2015–2016 at Changping (CP) or Shunyi (SY), and subjected to drought-stressed (DS), well-watered (WW) or heat-stressed (HS) conditions at either the jointing (J) or grain filling (G) stage. Error bars, ± SE. Statistical significance was determined by a two-sided *t*-test, * $P < 0.05$, ** $P < 0.01$, *** $P < 0.001$.

Generation of transgenic wheat

For gene overexpression lines, the coding sequence of *TaWAK5* was synthesized in its entirety (Sangon Biotech, China) and then inserted into the pWMB110 vector, which harbors the ubiquitin promoter. For gene knockout mutants, four primers were designed for the *TaWAK5* gene. Each primer contained two 19 bp specific sequences. Subsequently, the pCBC-MT1T2 fragments were inserted into the CRISPR/Cas9 vector pBUE414, with two guide RNAs for targeted modification. The immature embryos of the spring bread wheat cultivar Fielder were utilized for transformation, mediated by *Agrobacterium tumefaciens* EHA105, of the constructed vectors. Transgenic T_0, T_1 and T_2 wheat seedlings were screened using QuickStix Kit for PAT/*bar*. For real-time PCR detecting gene expression, the three-leaf wheat seedlings of *TaWAK5* overexpressed T_3 homozygous lines were employed. The targeting sites of *TaWAK5* knockout T_3 homozygous lines were identified through PCR and sequencing. Homozygous transgenic lines were chosen to conduct phenotypic observation. Primers are listed in Table S3.

Physiological experiments, OGs treatment and yield-related trait analysis

Seedling survival rate evaluation under drought conditions, stomatal aperture and yield-related traits were measured as described before [56]. Briefly, the seedlings at the three-leaf stage were deprived of water for 25 days. Survival rate was examined on the fifth day after re-watering. Using the seedlings before and after 2-week water deprivation as the plant materials, Arabic gum was applied on the abaxial epidermis of the second fully expanded leaf to observe stomata. The stomatal aperture was photographed under a microscope and measured by Image J software. Additionally, wild type, overexpression and knockout seedlings were sprayed with 200 $\mu g \cdot ml^{-1}$ OGs. Before and after 1 h treatment, stomatal aperture was detected through applying Arabic gum. For yield-related trait analysis, plants were cultivated in the field within a removable rain-off shelter for the drought stress (DS) treatment and in the corresponding well-watered (WW) plots in two growing seasons of 2022 and 2023. After the harvest, the numbers of spikes per plant, the number of grains per spike, and the thousand-grain weight were documented.

Subcellular localization

The coding sequence of *TaWAK5* was integrated into the pCAMBIA1300 vector, which harbors the CaMV 35S promoter and a GFP tag, via seamless DNA cloning at restriction enzyme sites of *Xba* I and *Kpn* I using In-Fusion® Snap Assembly Master Mix (638947, Takara, USA). The construct vector and empty GFP vector were transformed into *Agrobacterium* GV3101 and then infiltrated into 4-week-old tobacco leaves, separately. After a 48 h incubation, the GFP fluorescence signal was visualized using a Zeiss LSM880 confocal microscope. For plasmolysis, the samples were immersed in 0.8 M mannitol solution for 10 min, and then the plasmolysis was observed with the microscope. Primers are listed in Table S3.

Protopectin (water-insoluble pectin) extraction, fractionation and content detection

Protopectin extraction and content detection were performed according to the manufacturer's protopectin content assay kit instruction (BC3685, Solarbio, China). Briefly, 1 g of sample was pulverized into a fine powder using liquid nitrogen. The obtained powder was suspended in 1 ml of extraction buffer I and incubated at 95°C for 20 min. The cell wall residue was harvested through centrifugation, re-suspended in 1.5 ml extraction buffer I twice, then in 100% acetone twice. Starch was removed by treatment with 1 ml extraction buffer II for 15 h with rotation. After discarding the supernatant, the precipitate was incubated with 1 ml extraction buffer III. After centrifugation, the supernatant is the extracted protopectin.

The protopectin sample was first filtered with a 0.22 μm filter and then separated using a Superdex 75 10/300 GL (GE Healthcare) gel filtration column (FPLC) [11]. Gel media were pre-equilibrated using 0.1 M sodium acetate buffer. Subsequently, each sample was applied to a 24 ml column and subjected to elution at a flow rate of 0.5 ml/min. A total of forty-eight fractions, with each fraction containing 500 μl of elution, were harvested and assayed for protopectin content. A molecular weight size standard kit (SigmaAldrich, MWGF200) was employed to estimate the molecular mass.

Protopectin content was determined also according to protopectin content assay kit instruction (BC3685, Solarbio, China). Briefly, 25 μl of each fraction was combined with 200 μl detection solution I, treated at 90°C for 10 min, and cooled to room temperature. For the background absorbance control, each sample was combined with 25 μl detection solution II, while each sample was combined with 25 μl detection solution III as measured fraction. All samples were kept at room temperature for 30 min, after which the absorbance at 530 nm was determined. A series of concentrations of galacturonic acid was employed to generate a standard curve for calculating the sample content. The experiment was repeated three times.

OGs extraction and content determination

Endogenous OGs from cell wall material were isolated and quantified as previously described [23,38]. For matrix-assisted laser desorption/ionization time-of-flight mass spectrometry (MALDI-TOF MS) analysis, OGs were mixed with 2,5-dihydroxybenzoic acid (DHB) matrix at a ratio of 1:1 (v/v). The experiment was performed using a Bruker ultrafleXtreme instrument at the Institute of Biophysics, Chinese Academy of Sciences in Beijing. Data were collected and analyzed using FlexAnalysis software.

Protein expression and purification

The TaWAK5 N-terminal and C-terminal were fused into pGEX-4T1 vector carrying a GST tag via seamless DNA cloning at an *Eco*R I and *Sal* I restriction site, respectively. Briefly, proteins were induced in Transetta strains. Specifically, 0.5 mM IPTG was added, and the strains were cultured at 16°C and 75 rpm for 8 h. Subsequently, the culture was harvested by centrifugation at 6000 g for 10 min at 4°C. The resulting pellet was resuspended in PBS supplemented with PMSF and a protease inhibitor cocktail and then subjected to sonication for 10 min. Following centrifugation, the supernatant was subjected to an incubation process with Glutathione Resin (L00206, GenScript, China) at 4°C for 2 h. After the resin was washed three times with PBS, the bound proteins were eluted from the resin using a GSH buffer (composed of 50 mM Tris-HCl, pH 8.0, and 10 mM GSH).

The TaSLAC1 N-terminal and C-terminal were fused into pMAL-c5X vector carrying MBP tag via seamless DNA cloning at a *Not* I and *Eco*R I restriction site, separately. Briefly, proteins were expressed in BL21 (DE3) strains with 0.5 mM IPTG for 8 h at 28°C, 100 rpm. The culture was collected by centrifugation at 6000 g for 10 min at 4°C, re-suspended in PBS (with PMSF and cocktail) and sonicated for 10 min. After centrifugation, the supernatant was incubated with Anti-MBP Magnetic Beads (E8037S, NEB, China) for 2 h at 4°C. After being rinsed three times with PBS, the proteins were purified from the resin using a 10 mM maltose elution buffer. The concentration of the purified protein was determined at a wavelength of 595 nm using the Quick Start Bradford Dye Reagent (5000205, Bio-Rad, USA). BSA was employed to generate a standard curve for the measurement. Primers are listed in Table S3.

Interaction analysis of protein with pectin and OGs

Oligogalacturonides were obtained from 1% polygalacturonic acid (P3850, Sigma, USA) according to the protocol reported in previous studies [38,89]. WAK-pectin/OGs interactions were analyzed through a modified enzyme-linked immunosorbent assay (ELISA) as described previously following the manufacturer's ELISA kit instruction (SEKF-105, Solarbio, China) [23,38]. Briefly, microplates were pre-treated with polylysine-HBr for 1 h. Pectin or oligogalacturonides (OGs) at concentrations of 1, 5, and 10 μg, which were dissolved in coating buffer, were added to each well. The plates were then incubated overnight at 4°C to coat the wells. After that, the wells were blocked with blocking buffer. Next, 250 ng of recombinant TaWAK5 N-terminal protein was added to the wells. Subsequently, the wells were thoroughly washed three times to eliminate unbound protein. Afterward, a GST tag antibody (CW0084, CWBIO, China) was used as the primary antibody at a 1:1000 dilution, and goat anti-mouse horseradish peroxidase (HRP) (A21010, Abbkine, China) was employed as the secondary antibody at a 1:5,000 dilution. These antibodies were applied to detect the proteins that remained bound to the polysaccharides. Finally, the HRP substrate reagent and terminal reagent were utilized to measure the absorbance at 450 nm, aiming to quantify the protein bound to the polysaccharide.

Bimolecular fluorescence complementation (BiFC) assay

The CDS of *TaSLAC1* and *TaWAK5* was fused into the YCE or YNE vector at *Pac* I and *Spe* I restriction sites via seamless DNA cloning technology, and separately introduced into GV3101. These distinct constructs were combined and infiltrated into 4-week-old tobacco leaves. Approximately 48 h after infiltration, YFP signals were detected under a confocal laser-scanning microscope (Zeiss LSM880, Germany). Primers are listed in Table S3.

Co-immunoprecipitation (CoIP) assay

The CDS of *TaSLAC1* was fused into the pCAMBIA1300 vector, which contains the CaMV 35S promoter and a Flag tag, through seamless DNA cloning at *Xba* I and *Sal* I sites. The construct was introduced into GV3101 and distinct combinations were injected into tobacco leaves, separately. CoIP was carried out following the protocol described in a previous study [56]. Primers are listed in Table S3.

Kinase activity assay, in vitro phosphorylation assay and Phos-tag mobility shift assay

For protein kinase assays, 200 $\mu g \cdot ml^{-1}$ OGs or pectin was sprayed on 4-week-old tobacco leaves expressing the TaWAK5-GFP construct. Proteins were extracted 1 h post-treatment and separated on polyacrylamide gel and Phos-tag polyacrylamide gel.

Anti-GFP (dilute at 1:2000, AE030, ABclonal, USA) was used for detection of TaWAK5-GFP. In vitro phosphorylation assays were carried out as follows. The MBP-tagged TaSLAC1-N or TaSLAC1-C protein was incubated together with GST-tagged TaWAK5-C protein in a kinase reaction buffer. The total volume of the reaction system was 30 μl, and the reaction was conducted at 30°C for 60 min, either in the presence or absence of ATP. The reaction was terminated by the addition of an equal volume of 2 × SDS sample loading buffer. Once boiled at 95°C for 5 min, the proteins were resolved on polyacrylamide gel and Phos-tag polyacrylamide gel. The Phos-tag mobility shift assays were executed in accordance with the manufacturer's guidelines (AAL-10, Wako, Japan). The 10% Phos-tag gels were prepared with 50 mM Phos-tag and 50 mM $MnCl_2$. The polyacrylamide gel was stained using Coomassie brilliant blue R250. For the immunoblotting detection of the Phos-tag polyacrylamide gel, anti-MBP antibodies (diluted at 1:3000, CW0288, CWBIO, China) were employed.

TaWAK5 gene expression analysis

To detect effects of SNP-947 (G/A) at 947 bp of the *TaWAK5* promoter region on expression level of *TaWAK5*, ten randomly selected accessions' leaves at the three-leaf stage were harvested for each haplotype. Total RNA was extracted and real-time PCR was performed. The *TaGAPDH* and *Tubulin* genes were used as internal controls to normalize the data. Total RNA was isolated, and real-time PCR was conducted. The *TaGAPDH* and *Tubulin* genes served as internal reference genes to standardize the data.

Marker development

Based on the SNP-947 in the *TaWAK5* promoter region, a dCAPS marker was developed that contains a mismatched nucleotide to produce a restriction endonuclease site for *Xho* I. The first-round PCR product using genome-specific primers was used as the template for the second round of PCR. The second round PCR products were digested with restriction enzyme *Xho* I and separated by electrophoresis on 4% agarose gel. Primers are listed in Table S3.

Yeast one-hybrid assays

Yeast one-hybrid assays were performed to check the binding of bZIP transcription factor TaPAN to the *TaWAK5* promoter region. The CDS of *TaPAN* was integrated into the pB42AD vector via seamless DNA cloning at *Eco*R I. *Hap1/2* (from cv. Fielder) or *Hap3/4* (from cv. Chinese Spring) promoter region of Ta*WAK5* was fused into pLacZi to serve as the reporter gene plasmid. The pB42AD vector with or without *TaPAN* was co-introduced along with the reporter gene constructs into yeast strain EGY48 following standard yeast transformation protocols. The transformed yeast cells were cultured on a medium deficient in Ura and Leu and supplemented with x-α-gal. The interaction between TaPAN and *TaWAK5* promoter was assessed by LacZ staining [90]. Primers are listed in Table S3.

Dual-luciferase assay of transformed tobacco leaves

The CDS of *TaPAN* was fused into the effector vector pCAMBIA1300, where its expression was driven by the CaMV 35S promoter. *Hap1/2* (from Fielder) and *Hap3/4* (from Chinese Spring) promoter regions of *TaWAK5* were ligated into the reporter vector pGreen II 0800-LUC, respectively. The effector and reporter constructs were introduced together into GV3101 along with the pSoup helper plasmid. Forty-eight hours after infiltration, the activities of firefly luciferase (LUC) and Renilla luciferase (REN) were determined using the Dual-Glo® Luciferase Assay System (E2920, Promega) on a multimode reader (TriStar^2 S LB942). Promoter activity was calculated as the ratio of LUC to REN. The LUC-REN ratio in tobacco plants transformed with the empty vector (pCAMBIA1300/pGreen II 0800-LUC) was standardized to 1. Primers are listed in Table S3.

Canopy temperature of wheat

The whole wheat panel was cultivated across 20 distinct environments, which were defined by the combinations of year, location and treatment. These environments were established at two sites in Beijing: Changping (40°13′N, 116°13′E) and Shunyi (40°23′N, 116°56′E). The cultivation spanned two growing seasons from 2014 to 2016. The treatments included two water regimes: drought-stressed (DS) and well-watered (WW), either with or without heat stress (HS). Canopy temperature was measured at the jointing (J) and grain filling (G) stages [56].

Gene IDs

The sequence data in this article can be found in the WheatOmics database. Gene IDs are TaWAK5, TraesCS5A02G043600; TaSLAC1, TraesCS2A02G398000; TaPAN, TraesCS7A02G207100.

Compliance with ethics requirements

The authors declare that this study has fully complied with all relevant ethics requirements.

CRediT authorship contribution statement

Jingyi Wang: Conceptualization, Investigation, Writing – original draft. **Long Li:** Formal analysis, Data curation. **Chaonan Li:** Investigation, Visualization. **Matthew Reynolds:** Resources. **Manuel Spannagl:** Writing – review & editing. **Jörg-Peter Schnitzler:** Resources. **Yang Zhao:** Investigation. **Zilong Ma:** Investigation. **Jiemeng Xu:** Validation. **Xinguo Mao:** Funding acquisition. **Ruilian Jing:** Writing – review & editing, Supervision.

Declaration of competing interest

The authors declare that they have no known competing financial interests or personal relationships that could have appeared to influence the work reported in this paper.

Acknowledgements

We thank Dr. Genying Li (Shandong Academy of Agricultural Sciences, China) for her assistance with the generation of transgenic wheat plants; Dr. Jiaying Yang (Institute of Crop Sciences, Chinese Academy of Agricultural Sciences) for performing the fast protein liquid chromatography analysis; and Dr. Hanlei Yang (from the group of Prof. Yihua Zhou at the Institute of Genetics and Developmental Biology, Chinese Academy of Sciences, China) for providing suggestions on the determination of OGs levels. This research was supported by grants from the National Key R&D Program of China (2023YFF1000603), the earmarked fund for CARS-03, the National Natural Science Foundation of China (32061143040), and the Major Project on Agricultural Biobreeding of China (2023ZD04026).

Appendix A. Supplementary data

Supplementary data to this article can be found online at https://doi.org/10.1016/j.jare.2026.03.018.

References

[1] Godfray HC, Beddington JR, Crute IR, Haddad L, Lawrence D, Muir JF, et al. Food security: the challenge of feeding 9 billion people. Science 2010;327 (5967):812–8.
[2] Ray DK, Mueller ND, West PC, Foley JA. Yield trends are insufficient to double global crop production by 2050. PLoS One 2013;8(6):e66428.
[3] Tester M, Langridge P. Breeding technologies to increase crop production in a changing world. Science 2010;327(5967):818–22.
[4] Wang J, Li C, Li L, Reynolds M, Mao X, Jing R. Exploitation of drought tolerance-related genes for crop improvement. Int J Mol Sci 2021;22(19):10265.
[5] Editorial, Down-to-earth drought resistance. Nat Plants 2024;10(4):525-526.
[6] Bacete L, Schulz J, Engelsdorf T, Bartosova Z, Vaahtera L, Yan GQ, et al. THESEUS1 modulates cell wall stiffness and abscisic acid production in *Arabidopsis thaliana*. P Natl Acad Sci USA 2022;119(1):e2119258119.
[7] Cosgrove DJ. Catalysts of plant cell wall loosening. F1000Res 2016;5(1):7180.
[8] Vaahtera L, Schulz J, Hamann T. Cell wall integrity maintenance during plant development and interaction with the environment. Nat Plants 2019;5 (9):924–32.
[9] Ridley BL, O'Neill MA, Mohnen D. Pectins: structure, biosynthesis, and oligogalacturonide-related signaling. Phytochemistry 2001;57(6):929–67.
[10] Kohorn BD. The state of cell wall pectin monitored by wall associated kinases: a model. Plant Signal Behav 2015;10(7):e1035854.
[11] Wu Q, Li Y, Lyu M, Luo Y, Shi H, Zhong S. Touch-induced seedling morphological changes are determined by ethylene-regulated pectin degradation. Sci Adv 2020;6(48):eabc9294.
[12] Huerta AI, Sancho-Andres G, Montesinos JC, Silva-Navas J, Bassard S, Pau-Roblot C, et al. The WAK-like protein RFO1 acts as a sensor of the pectin methylation status in Arabidopsis cell walls to modulate root growth and defense. Mol Plant 2023;16(5):865–81.
[13] Feng W, Kita D, Peaucelle A, Cartwright HN, Doan V, Duan Q, et al. The FERONIA receptor kinase maintains cell-wall integrity during salt stress through Ca^{2+} signaling. Curr Biol 2018;28(5):666–75.
[14] Du J, Anderson CT, Xiao C. Dynamics of pectic homogalacturonan in cellular morphogenesis and adhesion, wall integrity sensing and plant development. Nat Plants 2022;8(4):332–40.
[15] Carter R, Woolfenden H, Baillie A, Amsbury S, Carroll S, Healicon E, et al. Stomatal opening involves polar, not radial, stiffening of guard cells. Curr Biol 2017;27(19):2974–83.
[16] Rui Y, Xiao C, Yi H, Kandemir B, Wang JZ, Puri VM, et al. POLYGALACTURONASE INVOLVED IN EXPANSION3 functions in seedling development, rosette growth, and stomatal dynamics in *Arabidopsis thaliana*. Plant Cell 2017;29 (10):2413–32.
[17] Yi HJ, Rui Y, Kandemir B, Wang JZ, Anderson CT, Puri VM. Mechanical effects of cellulose, xyloglucan, and pectins on stomatal guard cells of *Arabidopsis thaliana*. Front Plant Sci 2018;9(5):1566.
[18] Rui Y, Chen Y, Yi H, Purzycki T, Puri VM, Anderson CT. Synergistic pectin degradation and guard cell pressurization underlie stomatal pore formation. Plant Physiol 2019;180(1):66–77.
[19] Zhang T, Yu L, Wang Y, Li P, Feng X, Jian G, et al. Esterified-pectin-coupled polar stiffening controls grass stomatal opening. Nat Plants 2026;12(12):191–204.
[20] Kohorn BD, Kohorn SL. The cell wall-associated kinases,WAKs, as pectin receptors. Front Plant Sci 2012;3(8):88.
[21] Kohorn BD. WAKs; cell wall associated kinases. Curr Opin Cell Biol 2001;13 (5):529–33.
[22] He Z, Fujiki M, Kohorn BD. A cell wall-associated, receptor-like protein kinase. J Biol Chem 1996;271(33):19789–93.
[23] Decreux A, Messiaen J. Wall-associated kinase WAK1 interacts with cell wall pectins in a calcium-induced conformation. Plant Cell Physiol 2005;46 (2):268–78.
[24] Decreux A, Thomas A, Spies B, Brasseur R, Van Cutsem P, Messiaen J. In vitro characterization of the homogalacturonan-binding domain of the wall-associated kinase WAK1 using site-directed mutagenesis. Phytochemistry 2006;67(11):1068–79.
[25] Kohorn BD, Johansen S, Shishido A, Todorova T, Martinez R, Defeo E, et al. Pectin activation of MAP kinase and gene expression is WAK2 dependent. Plant J 2009;60(6):974–82.
[26] Wagner TA, Kohorn BD. Wall-associated kinases are expressed throughout plant development and are required for cell expansion. Plant Cell 2001;13 (2):303–18.
[27] Lally D, Ingmire P, Tong HY, He ZH. Antisense expression of a cell wall-associated protein kinase, WAK4, inhibits cell elongation and alters morphology. Plant Cell 2001;13(6):1317–31.
[28] Kohorn BD, Kobayashi M, Johansen S, Riese J, Huang LF, Koch K, et al. An Arabidopsis cell wall-associated kinase required for invertase activity and cell growth. Plant J 2006;46(2):307–16.
[29] Zuo W, Chao Q, Zhang N, Ye J, Tan G, Li B, et al. A maize wall-associated kinase confers quantitative resistance to head smut. Nat Genet 2015;47(2):151–7.
[30] Kohorn BD. Cell wall-associated kinases and pectin perception. J Exp Bot 2016;67(2):489–94.
[31] Tai Y, Li M, Chen G, Zhou M, Fan Y, Lei M, et al. Battle beneath the wall: Modulating cell wall-associated kinase (WAK) and WAK-likes (WAKLs) to cope with biotic and abiotic stresses in plants. Plant Cell Environ 2025;48 (11):8326–40.
[32] Verica JA, Chae L, Tong H, Ingmire P, He ZH. Tissue-specific and developmentally regulated expression of a cluster of tandemly arrayed cell wall-associated kinase-like kinase genes in Arabidopsis. Plant Physiol 2003;133(4):1732–46.
[33] Sun Z, Song Y, Chen D, Zang Y, Zhang Q, Yi Y, et al. Genome-wide identification, classification, characterization, and expression analysis of the wall-associated kinase family during fruit development and under wound stress in tomato (*Solanum lycopersicum* L.). Genes 2020;11(10):1186.
[34] Sivaguru M, Ezaki B, He ZH, Tong H, Osawa H, Baluska F, et al. Aluminum-induced gene expression and protein localization of a cell wall-associated receptor kinase in Arabidopsis. Plant Physiol 2003;132(4):2256–66.
[35] Meco V, Egea I, Ortiz-Atienza A, Drevensek S, Esch E, Yuste-Lisbona FJ, et al. The salt sensitivity induced by disruption of cell wall-associated kinase 1 (*SlWAK1*) tomato gene is linked to altered osmotic and metabolic homeostasis. Int J Mol Sci 2020;21(17):6308.
[36] Giarola V, Krey S, von den Driesch B, Bartels D. The *Craterostigma plantagineum* glycine-rich protein CpGRP1 interacts with a cell wall-associated protein kinase 1 (CpWAK1) and accumulates in leaf cell walls during dehydration. New Phytol 2016;210(2):535–50.
[37] Kohorn BD, Kohorn SL, Todorova T, Baptiste G, Stansky K, McCullough M. A dominant allele of Arabidopsis pectin-binding wall-associated kinase induces a stress response suppressed by MPK6 but not MPK3 mutations. Mol Plant 2012;5(4):841–51.
[38] Wu XW, Bacic A, Johnson KL, Humphries J. The role of *Brachypodium distachyon* wall-associated kinases (WAKs) in cell expansion and stress responses. Cells 2020;9(11):2478.
[39] Kanneganti V, Gupta AK. RNAi mediated silencing of a wall associated kinase, OsiWAK1 in *Oryza sativa* results in impaired root development and sterility due to anther indehiscence. Physiol Mol Biol Plants 2011;17(1):65–77.
[40] de Oliveira LFV, Christoff AP, de Lima JC, de Ross BCF, Sachetto-Martins G, Margis-Pinheiro M, et al. The wall-associated Kinase gene family in rice genomes. Plant Sci 2014;229(1):181–92.
[41] Dai Z, Pi Q, Liu Y, Hu L, Li B, Zhang B, et al. *ZmWAK02* encoding an RD-WAK protein confers maize resistance against gray leaf spot. New Phytol 2024;241 (4):1780–93.
[42] Czajkowska BI, Jones G, Brown TA. Diversity of a wall-associated kinase gene in wild and cultivated barley. PLoS One 2019;14(6):e0218526.
[43] Tripathi RK, Aguirre JA, Singh J. Genome-wide analysis of *wall associated kinase* (*WAK*) gene family in barley. Genomics 2021;113(1):523–30.
[44] Giovannetti M, Genre A. Walking on a tightrope: cell wall-associated kinases act as sensors and regulators of immunity and symbiosis. New Phytol 2024;242(5):1851–3.
[45] Zhang X, Jia S, He Y, Wen J, Li D, Yang W, et al. Wall-associated kinase *GhWAK13* mediates arbuscular mycorrhizal symbiosis and *Verticillium wilt* resistance in cotton. New Phytol 2024;242(5):2180–94.
[46] Guo F, Wu T, Xu G, Qi H, Zhu X, Zhang Z. TaWAK2A-800, a wall-associated kinase, participates positively in resistance to fusarium head blight and sharp eyespot in wheat. Int J Mol Sci 2021;22(21):11493.
[47] Ni J, Dong Z, Qiao F, Zhou W, Cao A, Xing L. Phylogenetic analysis of wall-associated kinase genes in Triticum species and characterization of *TaWAK7* involved in wheat powdery mildew resistance. Plant Dis 2024;108(5):1223–35.
[48] Liu Y, Liu D, Zhang H, Gao H, Guo X, Fu X, et al. Isolation and characterisation of six putative wheat cell wall-associated kinases. Funct Plant Biol 2006;33 (9):811–21.
[49] Feng W, Lindner H, Robbins 2nd NE, Dinneny JR. Growing out of stress: the role of cell- and organ-scale growth control in plant water-stress responses. Plant Cell 2016;28(8):1769–82.
[50] Anderson CM, Wagner TA, Perret M, He ZH, He D, Kohorn BD. WAKs: cell wall-associated kinases linking the cytoplasm to the extracellular matrix. Plant Mol Biol 2001;47(1–2):197–206.
[51] Ferrari S, Savatin DV, Sicilia F, Gramegna G, Cervone F, De Lorenzo G. Oligogalacturonides: plant damage-associated molecular patterns and regulators of growth and development. Front Plant Sci 2013;4(13):49.
[52] Brutus A, Sicilia F, Macone A, Cervone F, De Lorenzo G. A domain swap approach reveals a role of the plant wall-associated kinase 1 (WAK1) as a receptor of oligogalacturonides. PNAS 2010;107(20):9452–7.
[53] Denoux C, Galletti R, Mammarella N, Gopalan S, Werck D, De Lorenzo G, et al. Activation of defense response pathways by OGs and Flg22 elicitors in *Arabidopsis* seedlings. Mol Plant 2008;1(3):423–45.
[54] Xue Y, Wang J, Mao X, Li C, Li L, Yang X, et al. Association analysis revealed that *TaPYL4* genes are linked to plant growth related traits in multiple environment. Front. Plant Sci 2021;12:641087.
[55] Zhang Y, Zhao Y, Li T, Ni C, Han L, Du P, et al. TaPYL4, an ABA receptor gene of wheat, positively regulates plant drought adaptation through modulating the osmotic stress-associated processes. BMC Plant Biol 2022;22(1):423.
[56] Wang J, Li C, Li L, Gao L, Hu G, Zhang Y, et al. *DIW1* encoding a clade I PP2C phosphatase negatively regulates drought tolerance by de-phosphorylating TaSnRK1.1 in wheat. J Integr Plant Biol 2023;65(8):1918–36.
[57] Zhang Y, Wang J, Li Y, Zhang Z, Yang L, Wang M, et al. Wheat TaSnRK2.10 phosphorylates TaERD15 and TaENO1 and confers drought tolerance when overexpressed in rice. Plant Physiol 2023;191(2):1344–64.
[58] Wang J, Li Q, Mao X, Li A, Jing R. Wheat transcription factor TaAREB3 participates in drought and freezing tolerances in *Arabidopsis*. Int J Biol Sci 2016;12(2):257–69.

[59] Vahisalu T, Kollist H, Wang YF, Nishimura N, Chan WY, Valerio G, et al. SLAC1 is required for plant guard cell S-type anion channel function in stomatal signalling. Nature 2008;452(7186):487–91.
[60] Geiger D, Scherzer S, Mumm P, Stange A, Marten I, Bauer H, et al. Activity of guard cell anion channel SLAC1 is controlled by drought-stress signaling kinase-phosphatase pair. P Natl Acad Sci USA 2009;106(50):21425–30.
[61] Zhang Y, Zhao Y, Hou X, Zhang C, Wang Z, Zhang J, et al. Wheat TaPYL9-involved signalling pathway impacts plant drought response through regulating distinct osmotic stress-associated physiological indices. Plant Biotechnol J 2025;23(2):352–73.
[62] Ma S, Wang M, Wu J, Guo W, Chen Y, Li G, et al. WheatOmics: a platform combining multiple omics data to accelerate functional genomics studies in wheat. Mol Plant 2021;14(12):1965–8.
[63] Jiao C, Xie X, Hao C, Chen L, Xie Y, Garg V, et al. Pan-genome bridges wheat structural variations with habitat and breeding. Nature 2025;637 (8045):384–93.
[64] Hu X, Yang L, Ren M, Liu L, Fu J, Cui H. TGA factors promote plant root growth by modulating redox homeostasis or response. J Integr Plant Biol 2022;64 (8):1543–59.
[65] Gupta A, Rico-Medina A, Cano-Delgado AI. The physiology of plant responses to drought. Science 2020;368(6488):266–9.
[66] Lamers J, van der Meer T, Testerink C. How plants sense and respond to stressful environments. Plant Physiol 2020;182(4):1624–35.
[67] Gong Z, Xiong L, Shi H, Yang S, Herrera-Estrella LR, Xu G, et al. Plant abiotic stress response and nutrient use efficiency. Sci China Life Sci 2020;63 (5):635–74.
[68] Yuan F, Yang H, Xue Y, Kong D, Ye R, Li C, et al. OSCA1 mediates osmotic-stress-evoked Ca^{2+} increases vital for osmosensing in Arabidopsis. Nature 2014;514 (7522):367–71.
[69] Zhu JK. Abiotic stress signaling and responses in plants. Cell 2016;167 (2):313–24.
[70] Boeynaems S, Alberti S, Fawzi NL, Mittag T, Polymenidou M, Rousseau F, et al. Protein phase separation: a new phase in cell biology. Trends Cell Biol 2018;28 (6):420–35.
[71] Dorone Y, Boeynaems S, Flores E, Jin B, Hateley S, Bossi F, et al. A prion-like protein regulator of seed germination undergoes hydration-dependent phase separation. Cell 2021;184(16):4284–98.
[72] Shkolnik D, Nuriel R, Bonza MC, Costa A, Fromm H. MIZ1 regulates ECA1 to generate a slow, long-distance phloem-transmitted Ca^{2+} signal essential for root water tracking in Arabidopsis. PNAS 2018;115(31):8031–6.
[73] Orosa-Puente B, Leftley N, von Wangenheim D, Banda J, Srivastava AK, Hill K, et al. Root branching toward water involves posttranslational modification of transcription factor ARF7. Science 2018;362(6421):1407–10.
[74] Zhang H, Zhu J, Gong Z, Zhu JK. Abiotic stress responses in plants. Nat Rev Genet 2022;23(2):104–19.
[75] Li W, de Ollas C, Dodd IC. Long-distance ABA transport can mediate distal tissue responses by affecting local ABA concentrations. J Integr Plant Biol 2018;60(1):16–33.
[76] Choi WG, Miller G, Wallace I, Harper J, Mittler R, Gilroy S. Orchestrating rapid long-distance signaling in plants with Ca^{2+}, ROS and electrical signals. Plant J 2017;90(4):698–707.
[77] Takahashi F, Suzuki T, Osakabe Y, Betsuyaku S, Kondo Y, Dohmae N, et al. A small peptide modulates stomatal control via abscisic acid in long-distance signalling. Nature 2018;556(7700):235–8.
[78] Chen K, Li GJ, Bressan RA, Song CP, Zhu JK, Zhao Y. Abscisic acid dynamics, signaling, and functions in plants. J Integr Plant Biol 2020;62(1):25–54.
[79] Leftley N, Banda J, Pandey B, Bennett M, Voss U. Uncovering how auxin optimizes root systems architecture in response to environmental stresses. Cold Spring Harb Perspect Biol 2021;13(11):a040014.
[80] Ferrari S, Savatin DV, Sicilia F, Gramegna G, Cervone F, De Lorenzo G, et al. Plant damage-associated molecular patterns and regulators of growth and development. Front Plant Sci 2013;4(49).
[81] De Lorenzo G, Brutus A, Savatin DV, Sicilia F, Cervone F. Engineering plant resistance by constructing chimeric receptors that recognize damage-associated molecular patterns (DAMPs). FEBS Lett 2011;585(11):1521–8.
[82] Sinclair SA, Larue C, Bonk L, Khan A, Castillo-Michel H, Stein RJ, et al. Etiolated seedling development requires repression of photomorphogenesis by a small cell-wall-derived dark signal. Curr Biol 2017;27(22):3403–18.
[83] Herold L, Ordon J, Hua CL, Kohorn BD, Nürnberger T, Defalco TA, et al. *Arabidopsis* WALL-ASSOCIATED KINASES are not required for oligogalacturonide-induced signaling and immunity. Plant Cell 2024;37(1):koae317.
[84] Duan M, Sack L, Baird AS, Ma Z. Cell wall pectin reshapes leaf drought tolerance in dry forests. Nat Commun 2026;17(1):1529.
[85] Munarin F, Tanzi MC, Petrini P. Advances in biomedical applications of pectin gels. Int J Biol Macromol 2012;51(4):681–9.
[86] Hua D, Wang C, He J, Liao H, Duan Y, Zhu Z, et al. A plasma membrane receptor kinase, GHR1, mediates abscisic acid- and hydrogen peroxide-regulated stomatal movement in *Arabidopsis*. Plant Cell 2012;24(6):2546–61.
[87] Wang J, Li L, Li C, Yang X, Xue Y, Zhu Z, et al. A transposon in the vacuolar sorting receptor gene *TaVSR1-B* promoter region is associated with wheat root depth at booting stage. Plant Biotechnol J 2021;19(7):1456–67.
[88] Juliana P, Poland J, Huerta-Espino J, Shrestha S, Crossa J, Crespo-Herrera L, et al. Improving grain yield, stress resilience and quality of bread wheat using large-scale genomics. Nat Genet 2019;51(10):1530–9.
[89] Kohorn BD, Hoon D, Minkoff BB, Sussman MR, Kohorn SL. Rapid oligo-galacturonide induced changes in protein phosphorylation in Arabidopsis. Mol Cell Proteomics 2016;15(4):1351–9.
[90] Wang J, Wang R, Mao X, Zhang J, Liu Y, Xie Q, et al. RING finger ubiquitin E3 ligase gene *TaSDIR1-4A* contributes to determination of grain size in common wheat. J Exp Bot 2020;71(18):5377–88.